JOURNAL OF MORPHOLOGY 273:405–422 (2012)

# Musculoskeletal Morphology and Regionalization Within the Dorsal and Anal Fins of Bluegill Sunfish (*Lepomis macrochirus*)

**Brad A. Chadwell and Miriam A. Ashley-Ross***

*Department of Biology, Wake Forest University, Winston-Salem, North Carolina 27109*

*ABSTRACT* Ray-finned fishes actively control the shape and orientation of their fins to either generate or resist hydrodynamic forces. Because of the emergent mechanical properties of their segmented, bilaminar fin rays (lepidotrichia), and actuation by multiple muscles, fish can control the rigidity and curvature of individual rays independently, thereby varying the resultant forces across the fin surfaces. Expecting that differences in fin-ray morphology should reflect variation in their mechanical properties, we measured several musculoskeletal features of individual spines and rays of the dorsal and anal fins of bluegill sunfish, *Lepomis macrochirus,* and assessed their mobility and flexibility. We separated the fin-rays into four groups based on the fin (dorsal or anal) or fin-ray type (spine or ray) and measured the length of the spines/rays and the mass of the three median fin-ray muscles: the inclinators, erectors and depressors. Within the two ray groups, we measured the portion of the rays that were segmented vs. unsegmented and branched vs. unbranched. For the majority of variables tested, we found that variations between fin-rays within each group were significantly related to position within the fin and these patterns were conserved between the dorsal and anal rays. Based on positional variations in fin-ray and muscle parameters, we suggest that anterior and posterior regions of each fin perform different functions when interacting with the surrounding fluid. Specifically, we suggest that the stiffer anterior rays of the soft dorsal and anal fins maintain stability and keep the flow across the fins steady. The posterior rays, which are more flexible with a greater range of motion, fine-tune their stiffness and orientation, directing the resultant flow to generate lateral and some thrust forces, thus acting as an accessory caudal fin. J. Morphol. 273:405–422, 2012. 

KEY WORDS: median fin; fin ray; regionalization; *Lepomis*

## INTRODUCTION

Actinopterygian fishes can actively control the shape and curvature of their fins due to the unique design of the supporting bony fin-rays (Fig. 1). Named for this defining characteristic, ray-finned fishes are able to adjust the stiffness and curvature of individual fin-rays, known as lepidotrichia, allowing for fine-tuned manipulation of the fin surface and resulting fin conformation (McCutchen, 1970; Arita, 1971; Videler, 1977; Lauder, 2006; Alben et al., 2007).

Although detailed structural descriptions of lepidotrichia and their mechanical properties are available from only a few teleost species [gourami and goldfish (Haas, 1962); trout (McCutchen, 1970); tilapia (Videler, 1977; Geerlink and Videler, 1987) and bluegill sunfish (Alben et al., 2007)], the general structure of lepidotrichia has been found to be consistent across all ray-finned fishes examined (Goodrich, 1904; Eaton, 1945; Arita, 1971; Taft, 2011). Each lepidotrich is composed of two halves, or hemitrichia (Fig. 1D), located opposite each other on each side of the fin bound together by flexible collagen fibers (Haas, 1962; Videler, 1977). The proximal third of each hemitrich is a single piece of unsegmented bone, while the remaining portion, which is often branched, consists of several bony segments (Fig. 1B–E). The proximal end of each unsegmented bone expands to form the head, which articulates with the underlying endoskeletal fin supports and serves as the attachment sites for the muscles of the fin-ray (Figs. 1 and 2). The most distal segments are bound by an unmineralized extracellular matrix of collagenous fibrils, known as actinotrichia (Haas, 1962; Videler, 1977), which prevent the distal segments from being able to move relative to one another.

The complex arrangement described above, coupled with the mechanical properties of the composite materials comprising the structure, allows the fish to control the bending and stiffness of individual lepidotrichia. A force parallel to the long axis of the lepidotrich applied to one side

Contract grant sponsor: NSF (to M.A.A.-R.); Contract grant number: IBN-0316331.

*Correspondence to: Miriam A. Ashley-Ross, Department of Biology, Box 7325, Wake Forest University, Winston-Salem, NC 27109. E-mail: rossma@wfu.edu

Received 24 March 2011; Revised 2 August 2011; Accepted 11 September 2011

Published online 23 November 2011 in Wiley Online Library (wileyonlinelibrary.com)
DOI: 10.1002/jmor.11031

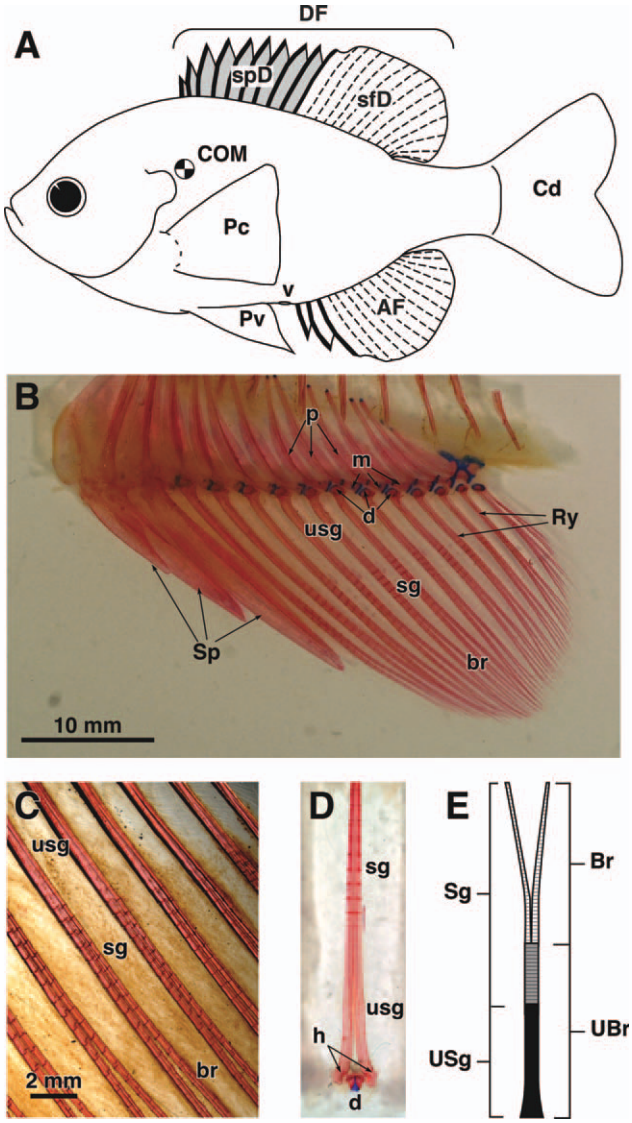


Fig. 1. **A:** Bluegill sunfish and its fins. The anterior spiny dorsal fin (spD; shaded region) is supported by 10 spines (thick, solid lines) with the most anterior spine positioned just above the center of mass (COM) and the soft dorsal fin (sfD) is supported by 13 rays (thin, broken lines). Although spD and sfD are developmentally independent, they appear as a single, continuous dorsal fin (DF) in bluegill. The single anal fin (AF), positioned just behind the vent (v), is supported by three spines and 13 rays. Fin-ray supports of the caudal fin (Cd) and the paired pectoral (Pc) and pelvic (Pv) fins are not shown. **B:** Photograph of a cleared and stained AF of *L. macrochirus*, viewed laterally, showing the external fin-ray supports [spines (Sp) and rays (Ry)] and endoskeletal supports [proximal (p), middle (m) and distal (d) radials]. The generalized design of lepidotrichia found in ray-finned fishes comprises three distinct regions: an unsegmented base (usg), a middle region of unbranched segments (sg) and a distal region of branched segments (br). **C:** Close-up of several rays and their three regions. **D:** Viewed caudally, the two hemitrichia (h) of a lepidotrich can be seen. The associated distal radial is positioned between the heads of the two usg bases. **E:** Schematic of a lepidotrich, viewed laterally, and its three regions: usg (solid black), sg (medium grey with striations), and br (light grey with striations). For comparative analyses, the three regions were combined into one of five variables: total RL (all three regions), USg vs. Sg (sg + br) or UBr (usg + sg) vs. Br.

displaces the two hemitrichia relative to one another, causing the ray to curve to one side and stiffen. Originally thought to be a passive reaction to hydrodynamic loading during swimming to prevent over-bending and to maximize propulsive thrust generated by the fins (McCutchen, 1970), later studies demonstrated that fish have a more active role in controlling the ray curvature and stiffness (Arita, 1971; Videler, 1977; Geerlink and Videler, 1987; Alben et al., 2007). Fish can activate fin muscles of the rays to not only reduce, or prevent, fin bending but to potentially modulate the hydrodynamic forces generated by actively controlling the shape and rigidity of the entire fin surface (Alben et al., 2007).

In the dorsal (DF) and anal (AF) fins, three paired muscles attach to the heads of both hemitrichia: the inclinator, erector, and depressor muscles (Winterbottom, 1974). Originating from the fascia between the skin and axial musculature, the inclinator inserts laterally onto the head and is responsible for lateral movement of the fin-ray (Fig. 2B). The erector and depressor muscles originate from

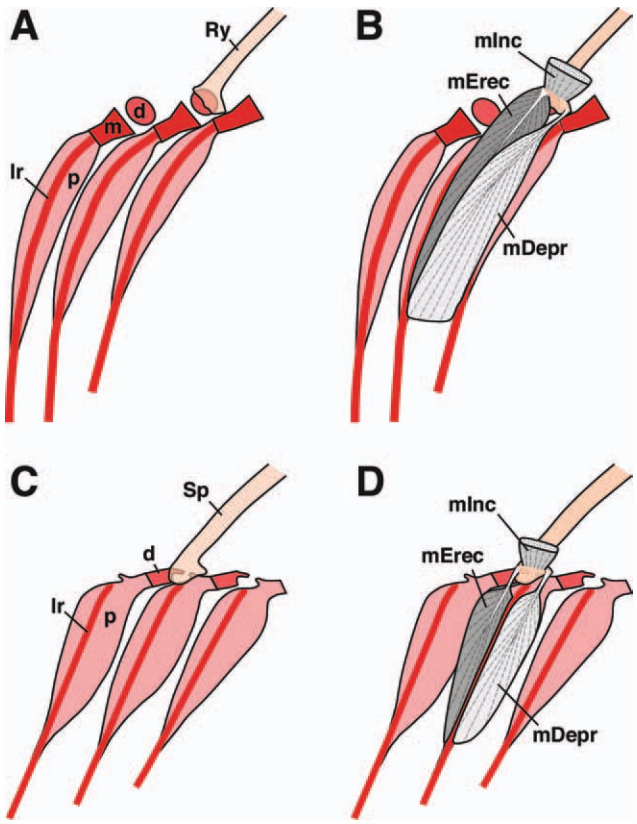


Fig. 2. Schematic of fin-ray joints and muscles. **A:** Ray-pterygiophore articulation; **B:** Muscles of the ray; **C:** Spine-pterygiophore articulation; and **D:** Muscles of the spine. Symbols: p (proximal radial); lr (lateral ridge); m (middle radial); d (distal radial); mInc (inclinator muscle, shown transected and reflected), mErec (erector muscle) and mDepr (depressor muscle).

the lateral surfaces of the rays' endoskeletal support (the pterygiophores) and insert onto anterolateral and posterolateral processes of the head (erector and depressor, respectively) and serve to erect or depress the fin-ray (Fig. 2B).

In derived teleost fishes, primarily within Acanthopterygii, specialized lepidotrichia composed of a single unbranched bony element, known as spines, support the anterior regions of the DF and AF (Fig. 1). Spines typically have the same complement of muscles attaching to them as lepidotrichia (Fig. 2D); however, spine movement is restricted primarily to elevation/depression, with little to no lateral deflection (Eaton, 1945; Geerlink and Videler, 1973). Widely accepted as an anti-predator device (Hoogland et al., 1956), the suggested role of the spines during locomotion is to act as a keel (providing lateral stability) and/or cutwater (smoothly dividing the flow of water to either side of the projecting fin; Eaton, 1945). However, to our knowledge, no study has investigated what hydrodynamic role, if any, spiny regions of the median fins play during swimming behaviors, with the exception of the observation that the orientation and velocity of flow at the region of the spiny dorsal fin does not change during slow swimming speeds (Drucker and Lauder, 2001).

Within the literature, the wide range of locomotor behaviors observed among ray-finned fishes has long been attributed to the variability in the anatomy and mechanics of the fins used for a particular swimming mode, e.g., undulation of the body and caudal fin vs. movement of the pectoral fins (see Blake, 2004; Walker, 2004; Lauder, 2006 for recent reviews). Despite the observations that fish are capable of controlling fin conformation depending on the swimming behavior employed, few studies have examined whether variations in fin-ray morphology within the fins exist and what effect they may have on their mechanical properties and/or kinematic parameters during locomotion (Arita, 1971; Standen and Lauder, 2005; Lauder and Madden, 2007; Taft et al., 2008).

In this study, we assess musculoskeletal traits of individual fin-rays of the DF and AF of *Lepomis macrochirus*, quantifying patterns of morphological variation between fin-rays, based on their position within the fins (location along the long axis of the body) and fin type (dorsal vs. anal). We hypothesized that 1) morphological patterns of the spines and rays would vary in a longitudinal fashion, reflecting the observed curved lateral profile of the fins (as seen in Fig. 1A) and differing movements during slow swimming; 2) soft DF and AFs would show symmetry in the musculoskeletal properties of the rays from equivalent longitudinal positions, as the fins have similar shapes and locations in front of the externally symmetrical homocercal tail, and have been shown to generate similar jets of water during swimming (Tytell, 2006); 3) the proportion of the fin ray demonstrating segmentation and branching would increase with longitudinal position (i.e., that anterior rays would show less, while posterior rays would show greater proportions that are segmented and/or branched), based upon observations that the trailing edges of fins are responsible for shedding vortices that impart momentum to the water (Tytell, 2006; Lauder and Madden, 2007) and generate jets that interact with the caudal fin (Tytell, 2006); 4) erector muscles associated with each fin spine/ray would be the largest in the anterior regions of the fin, while depressor muscles would be the largest in the posterior regions, to spread the fin membrane most effectively; and 5) muscle masses would correlate with the length of the spine or ray, as a longer spine or ray will require more force to move it. From cleared and stained specimens, we measured the total spine or ray length (RL), and the portion of each ray that was either unsegmented or segmented and branched or unbranched. From preserved specimens, we measured the mass of the three individual muscle slips of each spine and ray: the inclinators, erectors and depressors (Winterbottom, 1974), comparing both the individual masses of the three muscles among the fin-rays as well as the total mass of the three muscles.

From the morphological variation found between rays, we suggest they vary in their functional properties, altering the kinematic and hydrodynamic properties over the fin surface, and resulting in functional regionalization within the dorsal and anal fins.

## MATERIALS AND METHODS

### Animals

*L. macrochirus* Rafinesque, 1819 were acquired from a local fish hatchery (Foster Lake & Pond Management, Garner, NC) and maintained individually in 40 L tanks on a 12L:12D photoperiod at 23 ± 3°C. Sixteen individuals that showed no visible deformation or damage to their median fins were selected for this study, with standard length (SL, snout to caudal peduncle) ranging from 98 to 126 mm and body mass from 33.7 to 68.7 g. The DFs were supported by 9–10 spines and 13–14 lepidotrichia; AFs were composed of three spines and 12–13 lepidotrichia.

### Terminology

We follow the terminology established by Eaton (1945) when discussing the skeletal supports of the median fins. The term "rays" indicates lepidotrichia that remain segmented and capable of bending versus the modified lepidotrichia that have fused into spines (Fig. 1). The term "fin-rays" is used when referring to the external fin supports collectively and the distinction between rays and spines is ignored.

The pterygiophores provide the internal support of the DFs and AFs, their distal ends articulating with the head of the fin-rays. Each pterygiophore originates as a series of three cartilaginous radials, which may or may not fuse during ossification. When the radials remain separate, they are called the proximal, middle, and distal radials (or proximal and distal if only two persist) (Figs. 1B and 2).

Among acanthopterygians, two distinct dorsal fins develop: an anterior fin supported by spines and a posterior fin supported by rays, called the spiny and soft dorsal fins, respectively (Mabee et al., 2002). Although the dorsal fins of *L. macrochirus* appear as a single continuous fin, we maintain the distinction between spiny dorsal fin and soft dorsal fin (Fig. 1), as well as the division of the single AF into spines and rays.

## Fin Skeleton

Seven sunfish were cleared and stained for bone and cartilage (Song and Parenti, 1995) and digital images of the whole fish were taken (DiMage S404 digital camera; Minolta, Osaka, Japan). The DFs and AFs, including their ptyergiophores, were removed and examined under a stereomicroscope (Leica MZ16FA; Leica Microsystems, Heerbrugg, Switzerland) coupled with a digital camera (Retiga 4000R; Q-Imaging, Surrey, BC, Canada) and acquisition software (Image-Pro Plus v6.2; Media Cybernetics, Bethesda, MD). Digital images of the DFs and AFs were captured with the fins splayed and secured so that individual rays did not overlap. Illuminating the fins from underneath, the segmentation and branching patterns of the rays were easily distinguishable.

Digital images were imported into ImageJ (Rasband, 2008) for all measurements, with an object of known length in frame for scale. From images of the whole fish, SL was measured to take into account the shrinkage that occurs during the clearing and staining process (Mabee et al., 1998). From the close-up images of the fins, the lengths of three distinguishable regions of each lepidotrich were measured to the nearest 0.1 mm: the proximal, unsegmented region; the middle, segmented but unbranched region and the distal, segmented and branched region (Fig. 1D, E). As a single, unbranched bone, only the total lengths of the spines were measured.

From these regions, five skeletal variables were established for each ray (Fig. 1E): total ray length (RL; sum of all three regions), unsegmented (USg) vs. segmented length (Sg; middle + distal) and unbranched (UBr; proximal + middle) vs. branched length (Br). In addition to their absolute lengths, the relative segmented (rSg) and branched (rBr) lengths of each ray were calculated as percent of RL, allowing comparison among the rays independent of length. Finally, to evaluate the symmetry between the rays of the DFs and AFs, dorsal ray (DRy) values were subtracted from the corresponding anal ray (ARy) values (e.g., ARy1-DRy1, ARy3-DRy3, etc.) to calculate $\Delta X = X_{\mathrm{ARy}} - X_{\mathrm{DRy}}$ (where $X$ represents any variable, absolute or relative). For spines, total length (SpL) was the only variable measured and analyzed; due to the disparity in the number of spines and their longitudinal position (Fig. 1A), differences in the dorsal and anal spine (ASp) lengths were not analyzed.

Manipulations of the intact fins of preserved specimens were performed by hand before dissection to assess the mobility of the spines and rays at their joints. To test mobility, the base of the spine or ray was gripped with forceps and movement was attempted in the mediolateral and sagittal planes. Flexibility of individual fin-rays *in situ* was examined by pushing on each, and observing the resulting deflection. To evaluate the flexibility and connection between hemitrichia, individual rays were removed and the base of one hemitrich was held stationary while the other was gripped with forceps and force was applied along the long axis; the point at which curvature began and overall extent of ray bending was observed.

## Fin Muscles

From the remaining nine preserved fish, the muscles that actuate the fin-rays of the DFs and AFs were examined. With the exception of the last two rays of the sfD and AF (described below in Results section), each fin-ray was actuated by three pairs of muscle slips (Fig. 2B,D). Removing the skin surrounding the base of each fin exposed the inclinator muscle slips (mInc). Because mInc attaches to the underlying fascia of the skin, special care was required to prevent the accidental loss of these muscle slips during skinning. Erector and depressor muscle slips (mErec and mDepr, respectively) are located deep to mInc and the surrounding axial musculature, enclosed in a connective tissue sheath. Throughout the dissection, Weigert's solution was periodically applied to stain the myofibers, making it easier to distinguish between muscle and connective tissues.

From fish in which all muscle slips were still intact throughout the dissection, the mass of each individual muscle slip (left side only) was recorded to the nearest 0.1 mg with an electronic microgram scale. For each fin-ray, the masses of its three muscle slips were summed to get the total muscle mass (mTM). Similar to the skeletal variables, the relative mass of each muscle slip (rInc, rErec, and rDepr) was calculated as a percent of mTM and the difference between the paired DRy and ARy muscle masses were calculated ($\Delta X$).

## Statistical Analysis

To avoid complications resulting from empty cells, specimens that had only nine dorsal spines (DSps) or 12 ARys were excluded; in the few cases of individuals that had 14 DRys, the first anterior ray was removed from the analysis. Six cleared and stained specimens met this condition and were included for analysis of the skeletal variables. For the muscular analysis, five preserved specimens were included.

Fin-rays were assigned to one of four groups based on its fin-ray type (spine or ray) and fin (dorsal or anal): DSp, DRy, ASp, and ARy. Within each group, fin-rays of each individual were numbered according to its ranked longitudinal position within the fin, starting with the anteriormost fin-ray. A significant degree of heteroscedasticity within several variables, which was not eliminated even after a logarithmic or square root transformation, made ANOVAs inappropriate for this analysis and a series of nonparametric tests were used to examine the musculoskeletal variation within the four groups.

For the absolute and relative variables, position effects within each fin-ray group was tested using Friedman's method for randomized blocks ($\chi^2$), with each specimen as a block and its fin-rays as the treatment levels (Sokal and Rohlf, 1981; Zar, 1984). In addition, Kendall's coefficient of concordance ($W$) was calculated to estimate the degree of agreement in the rank order among fin-rays, providing a means to easily compare the consistency among fish. Ranging from 0 to 1, higher $W$ scores signify an increasing degree of concordance, with perfect consistency in rank order among all fish resulting in $W = 1$. Spearman's rank correlation ($r_s$) was calculated to assess the direction (positive or negative) and magnitude of the rank correlation between the positions of the fin-rays and their morphological features. Thus, tests of statistical significance are based upon the rank ordering of the parameters associated with the spines/rays, and not upon the raw values.

We also examined what, if any, differences in morphological patterns existed between DRy and ARy. For variables with significant position effects ($\chi^2$) within both ray groups, multigroup coefficients of concordance ($w$) were computed to test whether the observed position effect within the two fin groups were the same (Zar, 1984). Similar to $W$, increasing levels of agreement in rank order both within and between groups results in a $w$ coefficient that approaches 1; significant concordance between variables of the two fins was determined by comparing its $Z$-score (normal deviate) against the critical value ($Z_\alpha$) of the normal curve.

To test the hypothesis of symmetry between DRy and ARy, fin effects were tested by performing a two-tailed sign test on $\Delta X$ (both raw and relative values; Sokal and Rohlf, 1981; Zar, 1984). Position $\times$ fin interactions were examined by performing Friedman's method ($\chi^2$) on $\Delta X$ of all variables to look for variation in symmetry between the paired rays of DRy and ARy. The coefficient of concordance ($W$) and Spearman's rank correlation ($r_s$) were also calculated to facilitate the description of the interactions.

Using the average fin-ray lengths from the six cleared and stained specimens and the average mass of each muscle slip

from the five preserved fish, we calculated Pearson's product-moment correlation coefficients ($r$) between the spine/ray lengths (dorsal and anal) and mass of their three muscles. Although not a statistically valid comparison, as the fin-ray lengths and muscle masses were not measured from the same individuals, $r$ provides an estimate of the relationship between fin-ray length and muscle mass.

Custom written programs, based on the equations of Zar (1984), were developed in MatLab v7.6 (Mathworks, Natick, MA) to perform the sign test and the concordance between groups ($w$ and $Z$). All other statistical calculations were performed in SPSS v15.0 (Predictive Analytics SoftWare, Chicago, IL). It should be noted that because $W$ was calculated from the $\chi^2$ obtained from Freidman's method and shares the same $P$-value, the statistical interpretation for a trait's concordance and its position effect (or interaction) are equivalent. To control for Type I errors resulting from multiple comparisons of the skeletal (22) and muscular (49) characteristics, $P$-values were compared with corrected $\alpha$-levels using the sequential Bonferroni adjustment (Rice, 1989). As the majority of $P$-values were much less than the minimum adjusted $\alpha$-level for both sets of characteristics (ca. 0.001), this correction affected only a few of the tests.

## RESULTS

### Fin Skeleton

**Spines.** Spine length varied significantly with longitudinal position within DSp ($\chi^2 = 42.1$; $df = 5, 9$; $P < 0.001$) and ASp ($\chi^2 = 12.0$: $df = 5, 2$; $P < 0.001$). Among the three spines of the AF, average length (SpL) consistently increased posteriorly for all individuals, from ca. 15 to 25 mm, revealing complete concordance ($W = 1$) in the rank order of SpL among the fish and a perfect positive rank correlation ($r_s = 1$) between length and position (Figs. 3B and 4A). Within DSp, SpL also increased with position; however, a consistent increase in length occurred only among the anterior four spines, from ca. 7 to 19 mm. Among the posterior seven spines, average SpL remained similar, ca. 20 $\pm$ 1.5 mm (mean $\pm$ 1 s.d.), with no clear agreement in their rank order between individuals, resulting in a moderate degree of concordance and rank correlation, compared with that seen in ASp (Figs. 3A and 4A).

**Rays.** Located opposite each other at approximately the same longitudinal position along the body (Fig. 1), rays of the sfD and AF demonstrated similar patterns of changes in RLs, segmentation and branching (Figs. 3C–F and 4). As the mechanical behavior of any individual strut of bone is more likely to be influenced by its own segmentation or lack thereof (Alben et al., 2007), and not by the presence of a branch from it, we restricted our statistical analysis to USg vs. Sg, and did not test for significant differences in UBr vs. Br. For each of the four skeletal variables analyzed (RL, USg, Sg, and rSg), DRys and ARys at the same position within the fins show very little difference in their average lengths and had the same overall pattern in length changes with ray position (Fig. 4). Ray position had a significant effect on all four variables within both DRy and ARy ($\chi^2 > 35$; $df = 5, 12$; $P < 0.001$) and between the two ray groups ($Z > 10$; $P < 0.001$).

When ranked by absolute length, all three skeletal variables (RL, USg, and Sg) showed a high degree of concordance among individuals within DRy and ARy ($W > 0.80$). Among the variables analyzed, the relationship between ray position and length fell into one of two generalized patterns: a linear or a second order polynomial relationship (Fig. 4). Rank order of RL and USg lengths were highly correlated with position ($r_s$ ca. $-0.90$), with average lengths decreasing steadily with position within DRy and ARy (Figs. 3 and 4). However, unlike the nearly uniform decrease in length across all ray positions observed in USg, average RL initially increased slightly among the anterior two or three rays (Figs. 3 and 4). Within DRy, the decrease in RL among the middle rays was small, but progressed rapidly among the posterior rays (Fig. 3). In addition to strong position effects observed within DRy and ARy, patterns of RL and USg lengths also displayed high degrees of concordance between the two groups ($w \geq 0.95$; Fig. 4A,B).

The pattern of initial increase in RL mirrors that of Sg, which increased initially, reaching maximum length at the fourth to seventh ray. Posterior to that range, average lengths decreased, producing rank orders that more closely resembled second order polynomial curves than linear correlations (Figs. 3 and 4). Within ARy, Sg lengths were still moderately correlated with position ($r_s = -0.80$); however, within DRy, the rank correlation was much lower ($r_s = -0.60$). For the position effects detected within DRy and ARy, the degree of concordance between ray groups was high for Sg ($w = 0.88$; Fig. 4C).

Within DRy and ARy, rSg increased with position from ca. 50 to 75% among the first eight rays after which rSg gradually decreased back to ca. 60% (Fig. 4). This curvilinear position effect was supported by strong degrees of concordance both within DRy and ARy ($W > 0.8$) and between ray groups ($w = 0.77$; Fig. 4D).

The only significant fin effects were observed in $\Delta$USg (ARy > DRy) and $\Delta$rSg (DRy > ARy; Fig. 5A–D). However, significant position $\times$ fin interactions were found in $\Delta$RL, $\Delta$USg and $\Delta$Sg ($\chi^2 > 50$; $df = 5, 12$; $P < 0.0001$), with the ranked $\Delta X$ values negatively correlated with position ($-0.2 > r_s > -0.9$; Fig. 5E–G). These interactions were discernible such that ARy > DRy among the anterior rays, while ARy $\leq$ DRy posteriorly. No significant interactions were found for $\Delta$rSg ($\chi^2 > 25$; $df = 5, 12$; $P > 0.05$; Fig. 5H).

### Fin-Ray Articulation and Mobility

Similar to the arrangement described in the dorsal fin of tilapia (Geerlink and Videler, 1973), the

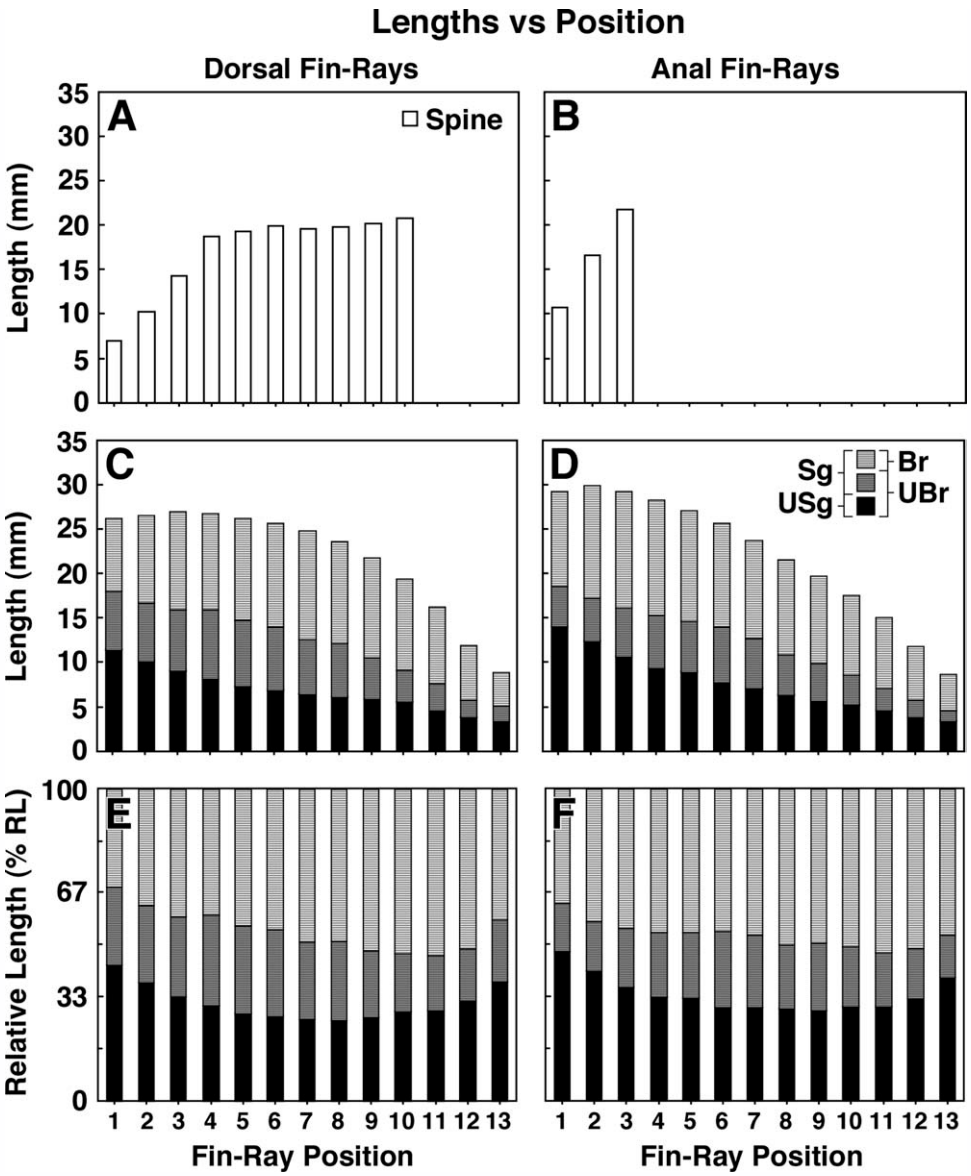


Fig. 3. Regional contribution to spine/ray length vs. position. **A, B:** Mean spine length (in mm) for DSp (10 spines) and ASp (three spines); **C, D:** Mean contribution to RL (in mm) of the usg base (solid black bars), sg (striated dark grey bars) and br (striated light grey bars) for DRy and ARy, respectively; and **E, F:** Mean relative contribution to RL (as a percent of total RL) of the three regions of DRy and ARy, respectively. The relationship between the lengths and longitudinal position of the rays can be compared, including the five tested variables: total RL (all three regions), USg (black bars) vs. Sg (all striated bars) and UBr (black + striated dark grey bars) vs. Br (striated light grey bars). Error bars not shown to improve clarity.

joint of each fin-ray (with exceptions for the first spine and last two rays) is formed by the distal radial of its corresponding pterygiophore and the proximal (or middle) radial of the subsequent pterygiophore (Fig. 2A,C). Although the components of the joints are similar between spines and rays, the arrangement of the components differ. Movements of individual fin-rays are also influenced by neighboring fin-rays, due to their connections via the fin membrane as well as a band of connective tissue between the proximal bases of adjacent fin-rays. Thus, any movement of a fin-ray, though actuated by its own musculature, can be influenced by the movement of adjacent rays. This is most readily observed when the elevation of one fin-ray causes all the posteriorly located fin-rays to elevate as well. Lateral movement of a single fin-ray also induced lateral movement among adjacent fin-rays, though this effect was less than for elevation.

**Spines.** The pterygiophore of each spine consists of proximal and distal radials, which are so closely associated that the distinction between the two was only possible under high magnification. The head of the spine is held securely in a socket

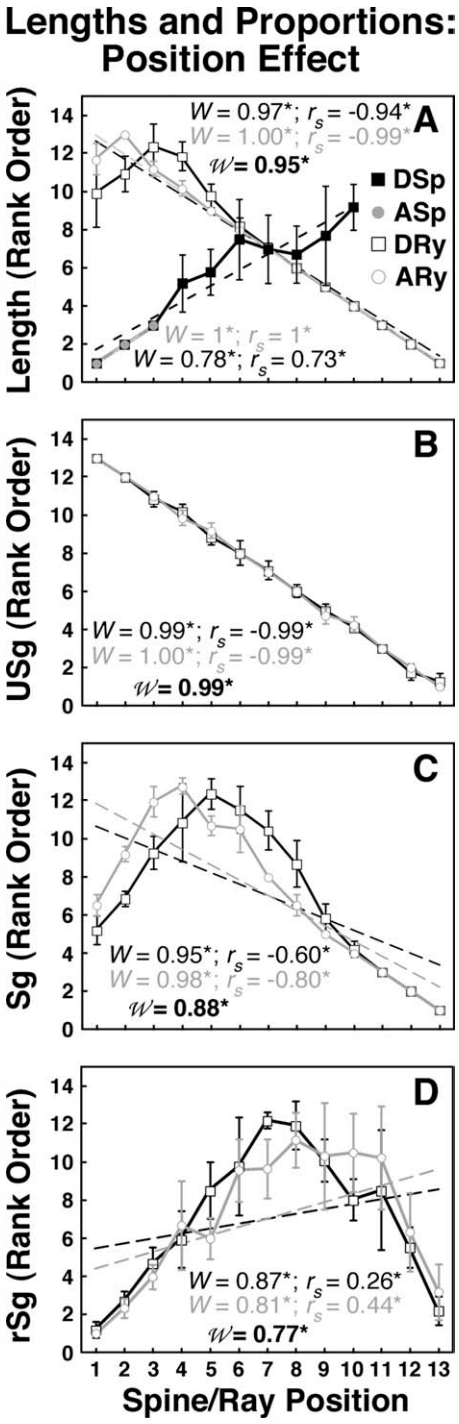


Fig. 4. Length vs. spine or ray position. **A:** Rank order of DSp, ASp, DRy, and ARy lengths; **B:** Rank order of USg length; **C:** Rank order of Sg length; and **D:** Rank order of relative segmented length (rSg). Numerical values provided are Kendall's coefficient of concordance ($W$; $df$ = 5, 12 for both fins) and Spearman's rank correlation ($r_s$) for DRy and ARy and the multigroup coefficient of concordance ($W$). Statistically significant $W$, $r_s$ and $W$ are indicated by an asterisk (*). Dashed lines represent the best-fit line (linear) between rank order and position. In panels A and B, one or both best-fit lines are completely, or partially, hidden by connecting lines due to a high degree of concordance and rank correlation between the regional length and position of the rays. Some error bars are concealed by their respective symbol ($n$ = 6 fish).

composed of its corresponding distal radial and the next proximal radial (Fig. 2C), forming the joint. In both fins, the first spine lacks its own pterygiophore, articulating instead on an expansion of the proximal radial corresponding with the second spine. A decrease in length and robustness of the proximal radials with spine position was the only discernable morphological difference noted.

Regardless of position, all spines could easily be elevated or depressed by manual manipulation. Although lateral motion was limited, the spines varied in the amount of force required to induce, and the extent of lateral deflection that could be attained. The three ASps and the anterior spines of spD were highly resistant to any lateral deflection. Lateral mobility among the posterior spines of spD increased slightly with position, though the degree of deflection by these spines did not approach that seen in the rays.

**Rays.** Unlike the spines, the number of radials that persist past ossification varied among the pterygiophores of the rays. Anteriorly, only the proximal and distal radials of rays #1–6 remained visually distinct and for the rest of the rays, all three radials (proximal, middle, and distal) persisted, though the proximal and middle radials were closely attached. Unlike the joints of the spines, the distal radial is loosely held in a socket formed by its corresponding middle (or proximal) radial and the next proximal/middle radial (Figs. 1B and 2A), which allows for the rotation of the distal radial about the long axis of the fish (i.e., lateral deflection). The two heads of the lepidotrich articulate on either side of the distal radial to complete the joint (Fig. 1D), which allows the ray to rotate within the median plane (i.e., elevate/depress), relative to the distal radial (Geerlink and Videler, 1973). Unlike the other rays, the last two rays (of both fins) articulate with the same distal radial and there is no "next" proximal radial to form the posterior edge of the socket (Fig. 1B). As with the spines, a decrease in length and robustness of the radials with ray position was observed. In addition, an increase in the distance between the distal radials and their socket can be observed in images of cleared and stained fins (Fig. 1B), suggesting that degree of mobility in the joint may increase with position.

During manipulations of intact fins and rays, all rays could be easily elevated and depressed; however, maximal degree of elevation decreased with axial position while maximal degree of depression increased. Compared with the spines, lateral deflection could easily be achieved although the degree of deflection increased with position while the amount of force needed to elicit the deflection decreased.

In isolated rays (i.e., removed from the fin), bending of most could be achieved by pulling on the head of one hemitrich while holding the other

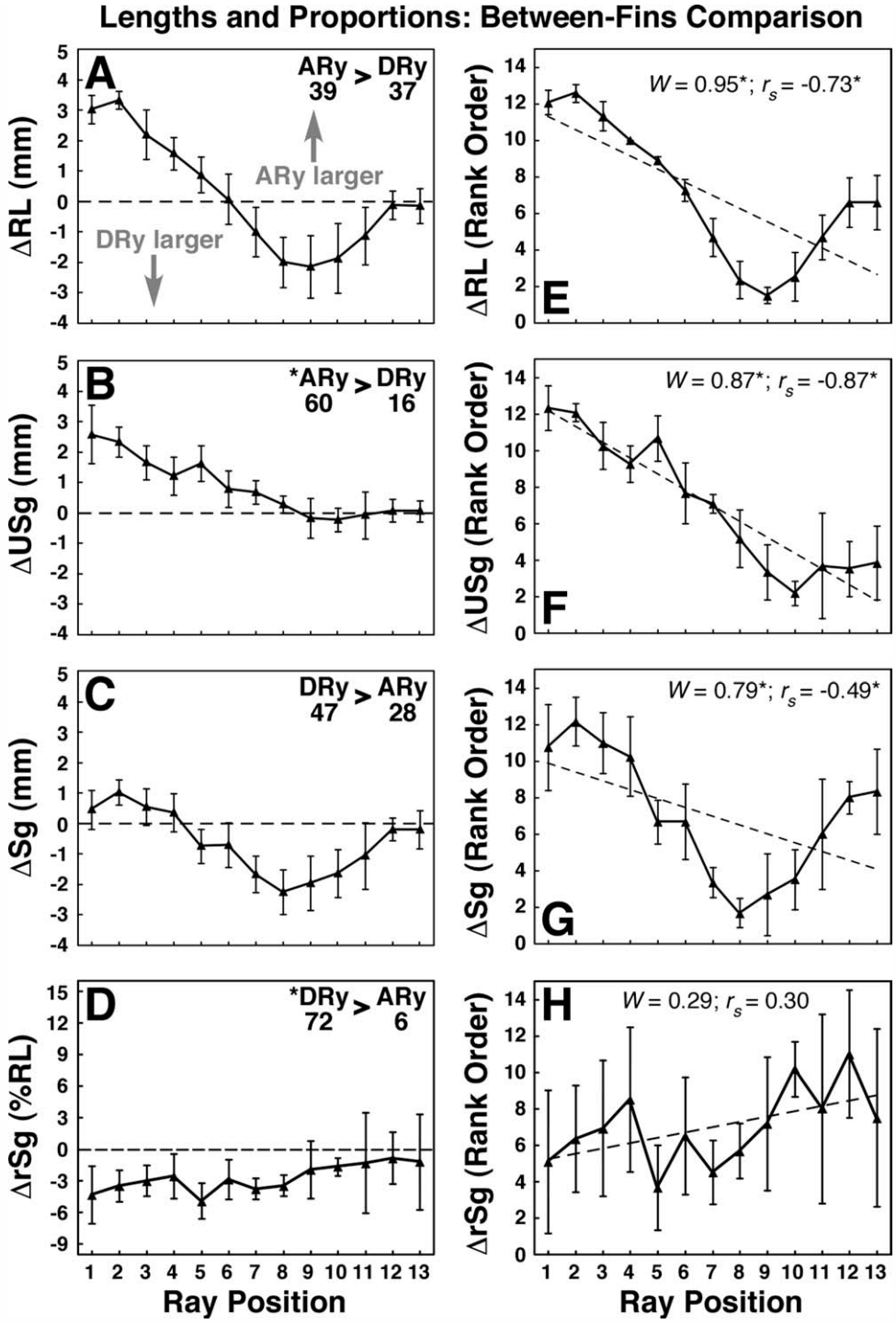


Fig. 5. Difference in regional lengths vs. position between dorsal and anal rays. **A:** Difference in total RL (ΔRL); **B:** Difference in USg length (ΔUSg); **C:** Difference in Sg length (ΔSg); **D:** Difference in relative segmented length (ΔrSg); **E:** Rank order of ΔRL; **F:** Rank order of ΔUSg; **G:** Rank order of ΔSg; and **H:** Rank order of ΔrSg. The values in the upper right corner of panels **A–D** specify the number of rays for each fin that were larger than the rays at the same longitudinal position from the other fin. Using the sign test, statistically significant fin effects are indicated by an asterisk (*). Symbols are mean ± 1 s.d. of ARy − DRy at similar longitudinal positions. Numerical values and interpretations in panels **E–H** as in Figure 4 ($df$ = 5, 12). For all panels, $n$ = 6 fish.

head stationary. For the first, second and, in some cases, third rays, bending could not be achieved by this method. During inspection of these rays, under a dissecting scope, it was noted that the proximal USg regions of the two hemitrichia were fused together and could not be moved relative to

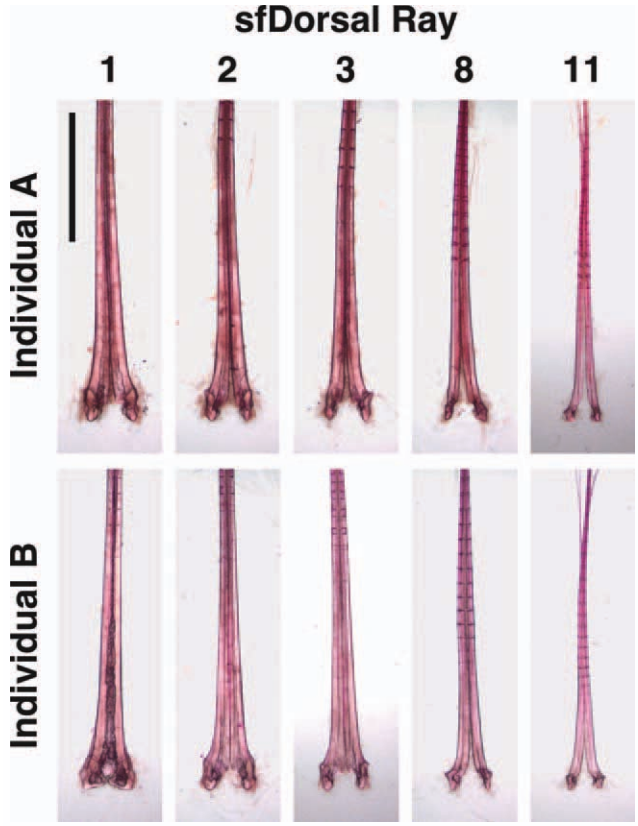


Fig. 6. Variation in attachment between hemitrichia. Caudal view of five isolated rays from the soft dorsal fin of two individual bluegill. Rigidity of attachment decreases from anterior to posterior, but individual fish vary.

each other. The degree of connection in these rays varied between specimens (Fig. 6), ranging from actual fusion of bone between the hemitrichia (Fig. 6, Individual B, ray 1), to collagenous fibers linking the hemitrichia so tightly that sliding movement was prevented. For the remaining rays, the ease with which ray bending could be elicited and the degree of curvature attained increased with position.

In comparing the rays of the DF and AF, the robustness of the pterygiophore and ray joint was greater among the anterior ARys compared with the anterior DRys. There was also a decrease in the joint mobility and ray flexibility in the anterior AF. No differences in the pterygiophore robustness, joint mobility or ray flexibility between the posterior DRys and ARys could be discerned.

## Fin Muscles

All fin-rays were actuated by three pairs of distinct muscle slips: mInc, mErec, and mDepr (Fig. 2B,D), with the exception of the last two rays of the DF and AF. In addition to sharing their articulation with the same distal radial (as described above), the last two rays shared the same fin musculature, as described in other species (Winterbottom, 1974). A single tendon of mInc appears to attach laterally to the heads of both rays. In addition, the bellies of this last pair of mErec and mDepr were fused together and could not be separated, as was easily done for all other fin-rays. A broad tendon from mErec/mDepr attaches to lateral processes on both heads of the rays, deep to the insertion of mInc.

Because of the peculiar muscular arrangement of this last pair of rays, the associated mErec and mDepr muscle slips were discarded from analysis, leaving 12 position levels for mTM and mInc, and 11 for mErec and mDepr (rather than the 13 levels seen in the skeletal analysis). As each spine was actuated by its own muscle slips, the number of position levels for DSp and ASp were the same as in the skeletal analyses (10 and 3, respectively).

**Spines.** For both DSp and ASp, mErec was the largest of the three muscle slips, contributing 50 to 75% of the total mass for each spine (Figs. 7 and 8). Within ASp, there was a high degree of concordance ($W > 0.75$) in the ranking of the absolute muscle mass; however, due to the small number of position levels, the $P$-values obtained exceeded the adjusted $\alpha$-level and the observed position effects were con-

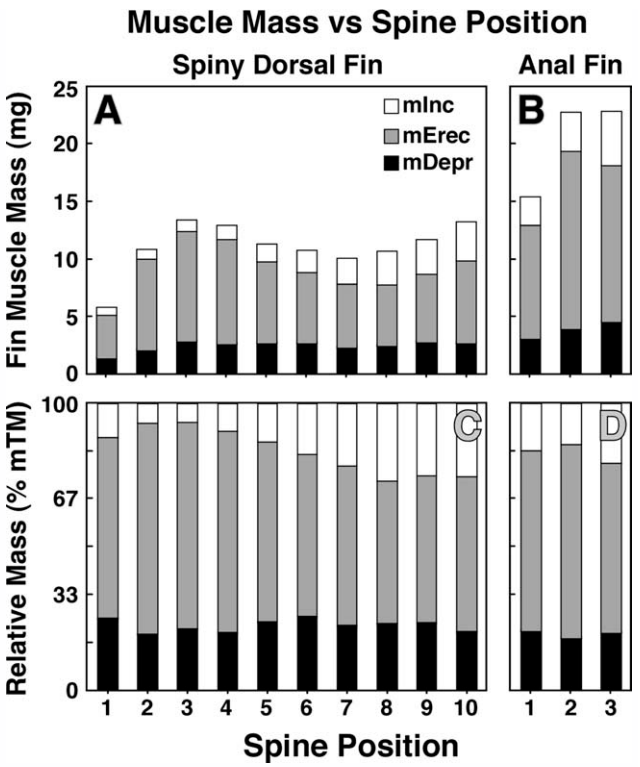


Fig. 7. Contribution to fin-ray muscle mass vs. spine position. **A, B:** Mean contribution to fin-ray muscle mass (in mg) from the three muscle slips of DSp and ASp, respectively: inclinator (mInc; open bars), erector (mErec; grey bars) and depressor (mDepr; black bars). **C, D:** Mean relative contribution to fin-ray muscle mass (as a percent of total fin-ray muscle mass; % mTM) from mInc, mErec and mDepr of DSp and ASp, respectively. Error bars not shown to improve clarity.

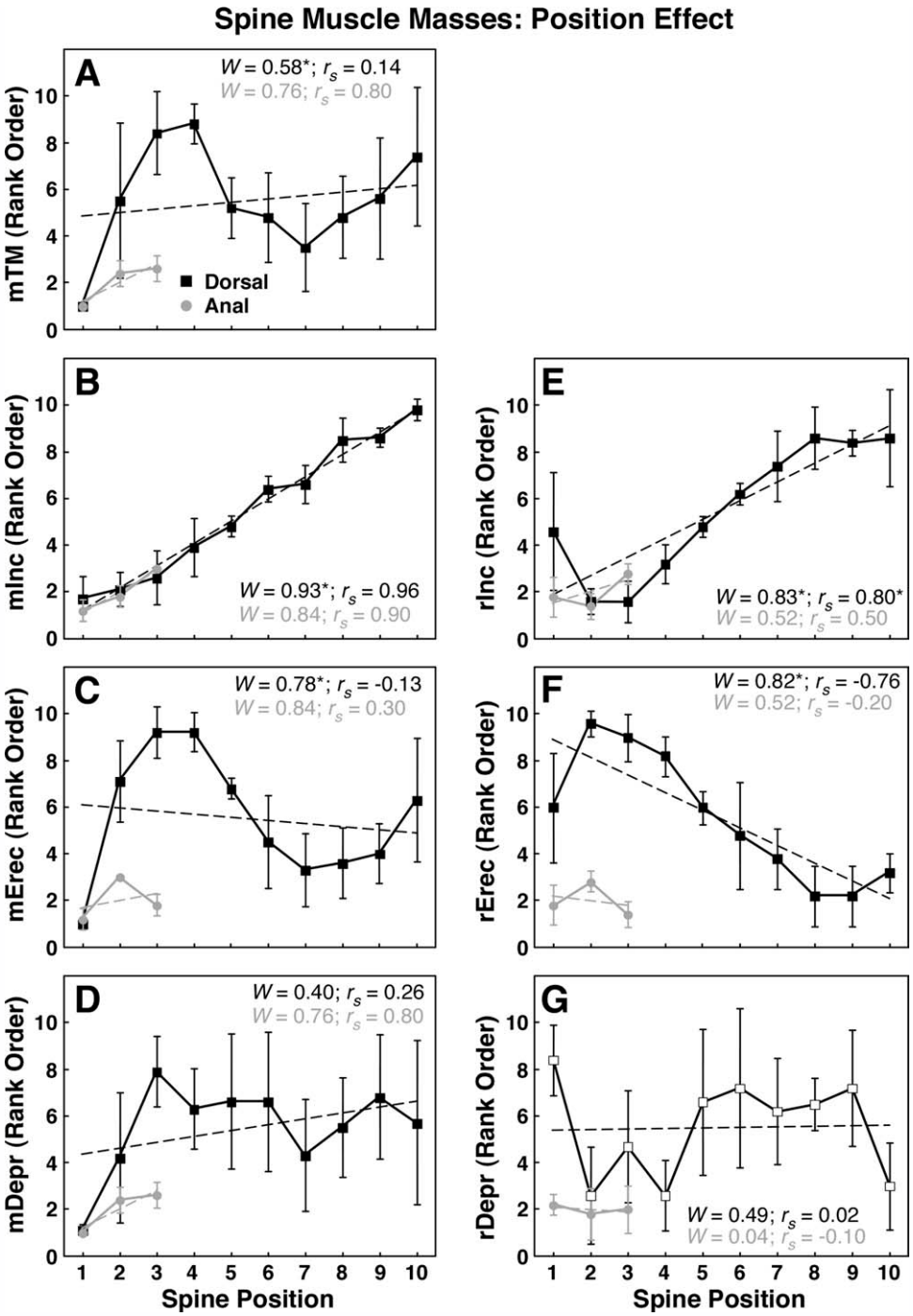


Fig. 8. Absolute and relative fin-ray muscle mass vs. spine position. **A:** Rank order of total muscle mass (mTM); **B:** Rank order of inclinator muscle mass (mInc); **C:** Rank order of erector muscle mass (mErec); **D:** Rank order of depressor muscle mass (mDepr); **E:** Rank order of relative inclinator muscle mass (rInc); **F:** Rank order of relative erector muscle mass (rErec); and **G:** Rank order of relative depressor muscle mass (rDepr). Symbols in all panels, and numerical values and interpretations as in Figure 4 ($df$ = 4, 9 and 4, 2 for DSp and ASp, respectively). For all panels, $n$ = 5 fish.

cluded to be nonsignificant ($\chi^2 > 7.5$; $df$ = 4, 2; $P >$ adjusted α-level; Fig. 8). In contrast, the relative distribution of the spine musculature (rInc, rErec and rDepr) within ASp was similar among the three positions, demonstrating no position effect ($\chi^2 \leq 5.2$; $df$ = 4, 2, $P \geq 0.075$; Fig. 8).

Within DSp, the depressor muscles (whether expressed as absolute or relative mass) showed no significant position effect ($\chi^2 < 25$; $df$ = 4, 9; $P >$ adjusted α-level; Fig. 8D,G). In contrast, significant position effects on the mass of inclinator and erector muscles (both absolute and relative

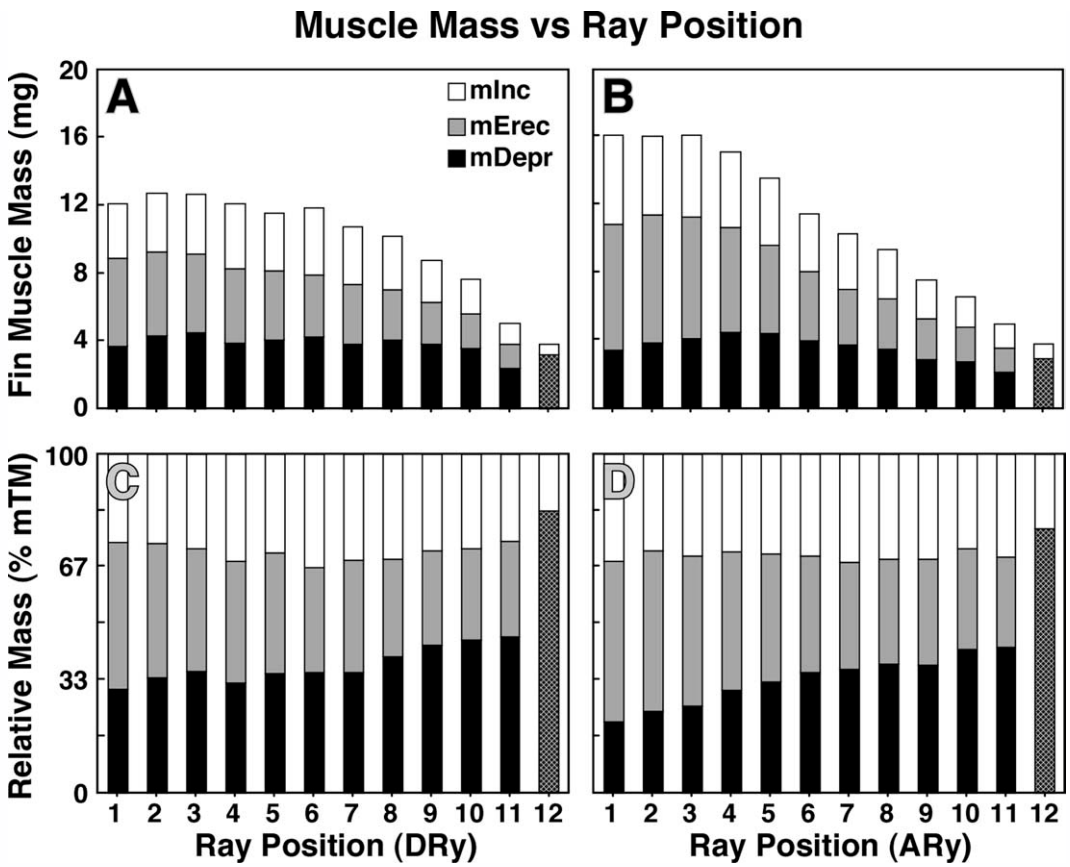


Fig. 9. Contribution to fin-ray muscle mass vs. ray position. **A, B:** Mean contribution to fin-ray muscle mass (in mg) from the three muscle slips of DRy and ARy, respectively: inclinator (mInc; open bars), erector (mErec; grey bars) and depressor (mDepr; black bars). For the two most posterior fin rays, mErec and mDepr are fused as a single muscle slip and their combined mass is provided (hatched bars); see text for details. **C, D:** Mean relative contribution to fin-ray muscle mass (as a percent of total fin-ray muscle mass; % mTM) from mInc, mErec and mDepr of DRy and ARy, respectively. Error bars not shown for clarity.

measures) were found ($\chi^2 > 35$; $df = 4, 9$; $P < 0.001$; Fig. 8B–F). Both mInc and rInc had a strong positive rank correlation with spine position ($r_s = 0.96$ and 0.80, respectively; Fig. 8B,E). Although rErec had a strong negative rank correlation with position ($r_s = -0.76$; Fig. 8F), mErec was not correlated with position ($r_s$ −0.13); rather, its distribution would be better fit with a third order polynomial curve (Fig. 8C). Combined, total mass of the spine musculature (mTM) had a significant position effect ($\chi^2 = 26.3$; $df = 4, 9$; $P = 0.0018$); as seen in mErec, mTM fit a third order polynomial curve rather than a directional rank correlation ($r_s = 0.14$; Fig. 8A).

**Rays.** Unlike mErec of the spines, there was not one specific ray muscle that consistently contributed the majority of total muscle mass at all ray positions for either DRy or ARy; instead, the three muscles of each were closer in mass (Figs. 9 and 10). With the exceptions of mDepr ($\chi^2 > 23.8$; $df = 4, 10$; $P >$ adjusted $\alpha$-level) of the DRy, ray position had a significant effect on the absolute mass of each muscle ($\chi^2 > 30$; $df = 4, 11/10$; $P < 0.001$), showing a high degree of concordance ($W > 0.75$) and a moderate to strong negative rank correlation with position (-0.4 > $r_s$ > -.98; Fig. 10). Ray position had significant effects on rErec and rDepr of both fins ($\chi^2 > 38$; $df = 4, 10$; $P < 0.001$), with rErec negatively correlated and rDepr positively correlated with position ($|r_s| \geq 0.8$; Fig. 10). For the five parameters in which position had a significant effect on muscle mass for both fin groups (mTM, mInc, mErec, rErec and rDepr), a significant degree of concordance between DRy and ARy was also found ($Z > 10$; $df = 4, 11/10$; $P < 0.001$; Fig. 10).

Of the seven $\Delta X$ parameters, significant fin effects were found in only two: ΔrErec (ARy > DRy) and ΔrDepr (DRy > ARy; Figs. 11 and 12). Significant position × fin interactions were found in three: ΔmTM, ΔmInc, and ΔmErec ($\chi^2 > 30.8$; $df = 4, 11/10$; $P <$ adjusted $\alpha$-level), with each parameter negatively correlated with position (Fig. 11). As seen in the skeletal parameters described earlier, the interactions were observed as the muscle mass of the anterior rays were larger in the AF, while posteriorly the muscle masses were equal or larger in the DRys (Figs. 11 and 12).

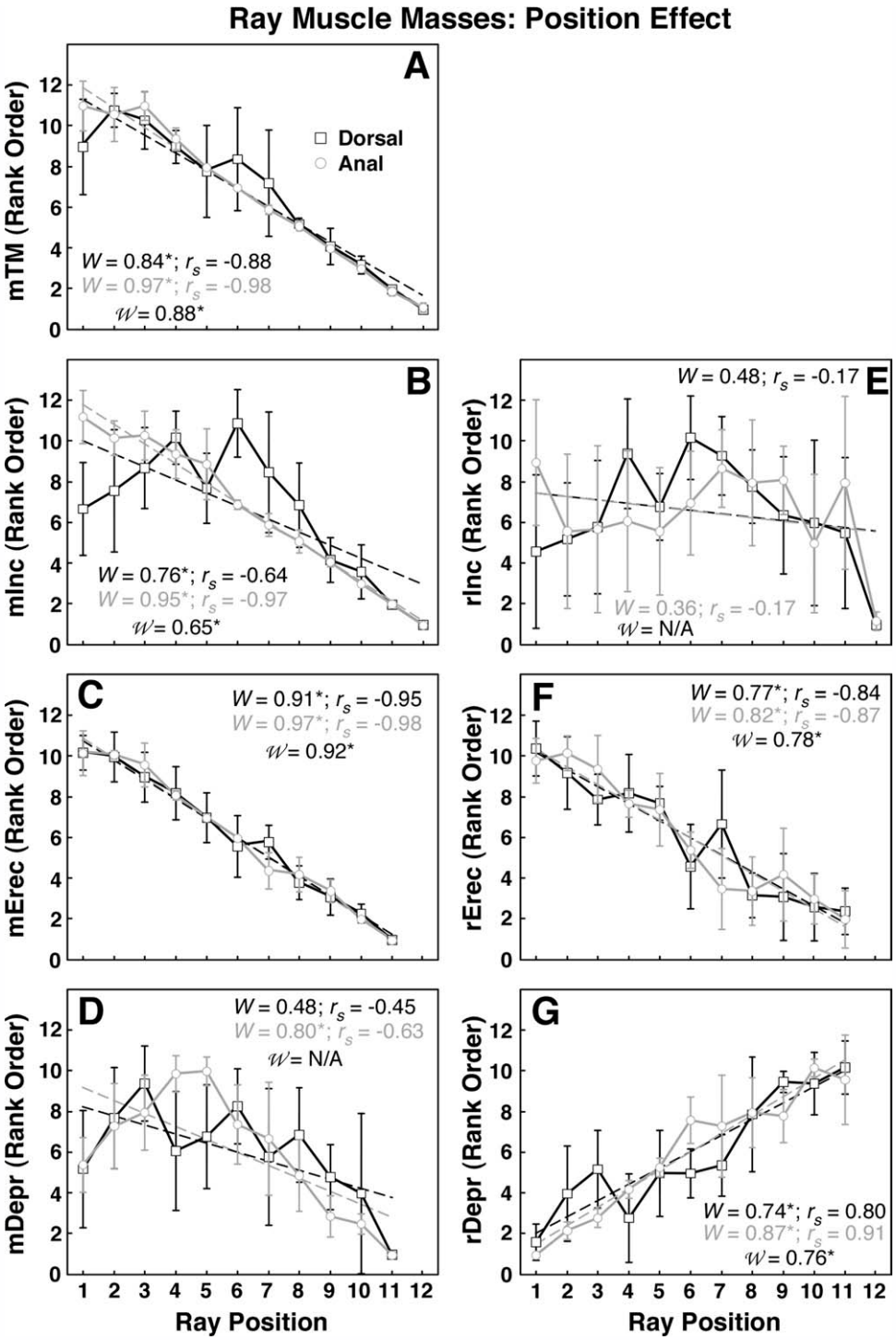


Fig. 10. Absolute and relative fin-ray muscle mass vs. ray position. **A:** Rank order of total fin-ray muscle mass (mTM); **B:** Rank order of inclinator muscle mass (mInc); **C:** Rank order of erector muscle mass (mErec); **D:** Rank order of depressor muscle mass (mDepr). **E.** Rank order of relative inclinator muscle mass (rInc); **F:** Rank order of relative erector muscle mass (rErec); and **G:** Rank order of relative depressor muscle mass (rDepr). Symbols in all panels, and numerical values and interpretations as in Figure 4 ($df$ = 4, 11 for mTM and mInc, $df$ = 4, 10 for mErec and mDepr). For all panels, $n$ = 5 fish.

### Fin-Ray Length Versus Muscle Mass

Among the spines of the DF and AF, only mInc showed a moderately positive correlation with spine length ($r^2$ = 0.39), while mErec and mDepr were only weakly correlated ($r^2$ = 0.01 and 0.22, respectively; Fig. 13A). However, all three

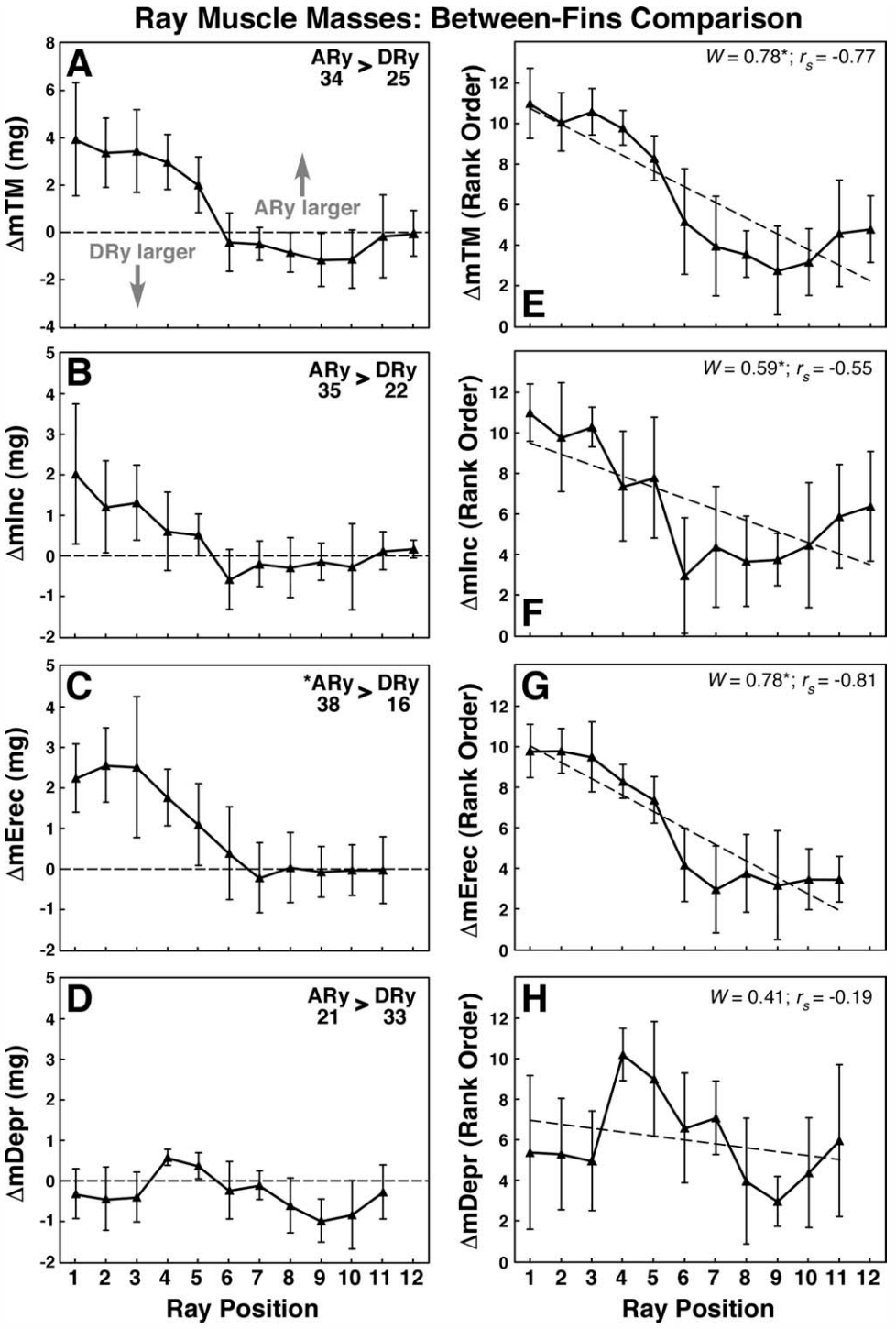


Fig. 11. Difference in fin-ray muscle mass vs. position between dorsal and anal rays. **A:** Difference in total fin-ray muscle mass (ΔmTM); **B:** Difference in inclinator muscle mass (ΔmInc); **C:** Difference in erector muscle mass (ΔmErec); **D:** Difference in depressor muscle mass (ΔmDepr). Positive values indicate ray positions where the muscle mass of ARy was greater than DRy; **E:** Rank order of ΔmTM; **F:** Rank order of ΔmInc; **G:** Rank order of ΔmErec; **H:** Rank order of ΔmDepr. Symbols in all panels, and numerical values and interpretations in panels **E–H** as in Figure 5 ($df$ = 4, 11 for mTM and mInc, $df$ = 4, 10 for ΔmErec and ΔmDepr). For all panels, $n$ = 5 fish.

muscle masses were highly correlated with total lengths of the dorsal and anal rays ($r^2 > 0.6$; Fig. 13B).

## DISCUSSION

During any fish behavior, whether it be station holding, maneuvering or swimming, three potential

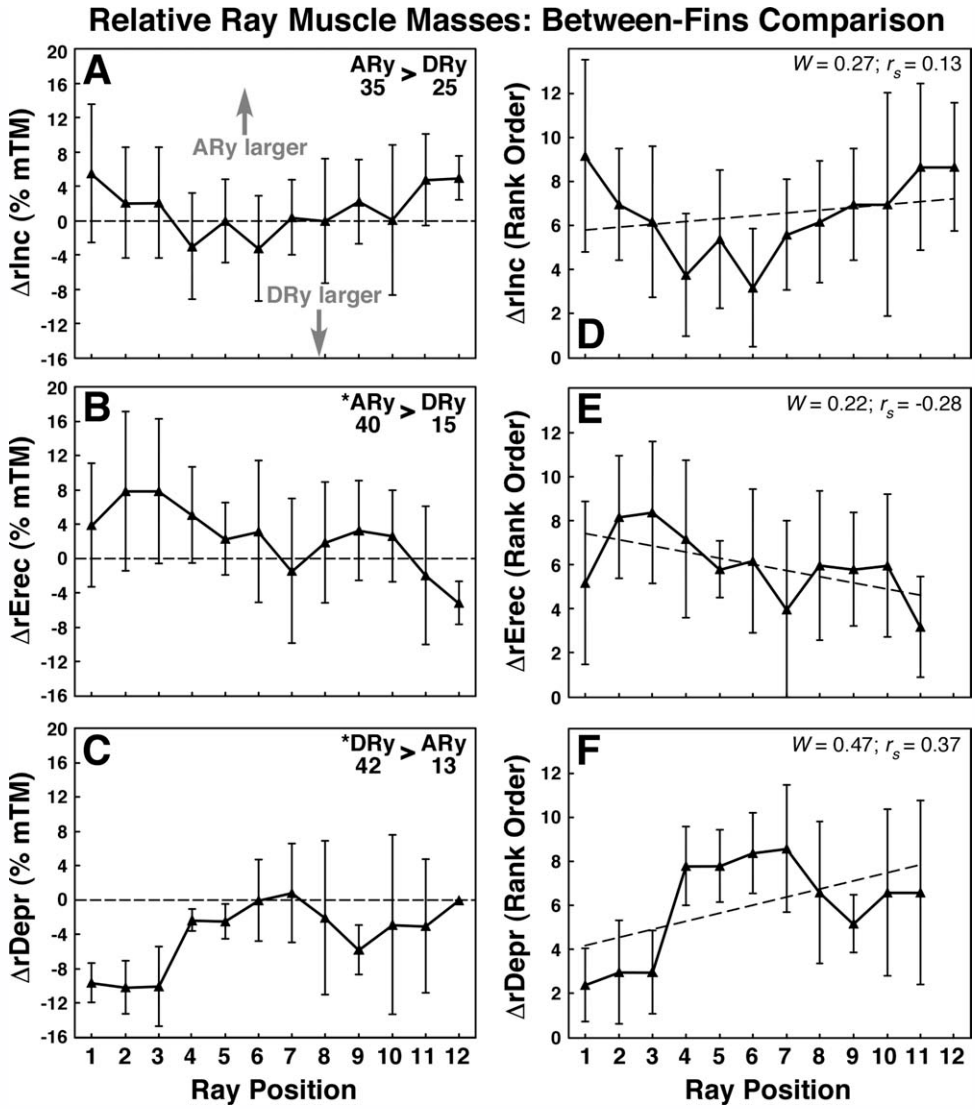


Fig. 12. Difference in relative fin-ray muscle masses vs. ray position. **A:** Difference in relative inclinator muscle mass (ΔrInc); **B:** Difference in relative erector muscle mass (ΔrErec); **C:** Difference in relative depressor muscle mass (ΔrDepr). Positive values indicate ray positions where the muscle mass of ARy was greater than DRy; **D:** Rank order of ΔrInc; **E:** Rank order of ΔrErec; **F:** Rank order of ΔrDepr. Symbols in all panels, and numerical values and interpretations in panels **D–F** as in Figure 5 ($df$ = 4, 11 for ΔrInc, $df$ = 4, 10 for ΔrErec and ΔrDepr). For all panels, $n$ = 5 fish.

sources of force can act on a ray or spine: 1) External forces; primarily hydrodynamic, generated from the interaction of the surrounding fluid (or solid substrate) with the fin surface; 2) Intrinsic muscular force; generated by the musculature of the individual fin-ray; and 3) Intra-fin forces; exerted on a fin-ray by the movement, or resistance, of neighboring fin-rays within a fin, transmitted by the fin webbing. The mechanical properties of a fin-ray, resulting from its structural design and material properties, determine how resistant or susceptible it is to these forces. Therefore, the interaction between a fin-ray's mechanical properties and the resultant force (the summation/negation of the forces listed above) ultimately determine its orientation and shape.

From the variations in the musculoskeletal features we measured and observed, we suggest that within the soft dorsal and anal fins and the spiny dorsal fin, fin-rays will differ in their resistance/susceptibility to different applied forces. For example, a ray that consists mostly of tightly bound, USg hemitrichia will deflect in response to external forces, but resist bending by muscular actuation. Moreover, as discussed below, there is regionalization of musculoskeletal properties within the three fins, suggesting different functional roles during locomotion.

## Skeletal Regionalization

We proposed three hypotheses regarding skeletal parameters of the DF and AF, which were

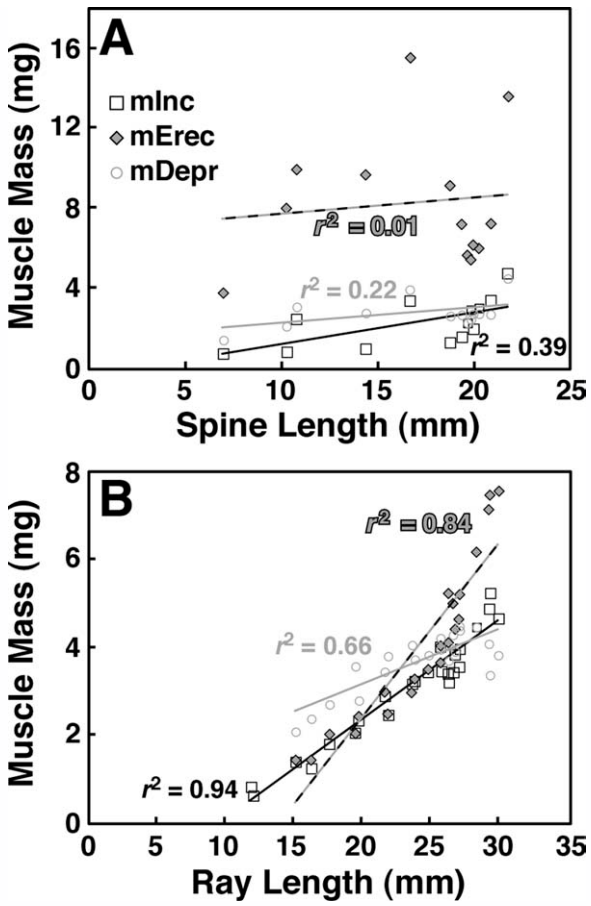


Fig. 13. Muscle mass vs. fin-ray length. **A:** Muscle mass vs. spine length; **B:** Muscle mass vs. ray length. Lines represent the best-fit line (linear) and the correlation ($r^2$) between the average fin-ray lengths ($n$ = 6 fish) and the average muscle masses ($n$ = 5 fish).

supported by significant position effects for all parameters measured, in both spiny and soft portions of the fins (Figs. 3 and 4). Lengths of bony elements first increased, then decreased as one moved from anterior to posterior in all fins. Further, segmentation increases with position in both soft fins, but decreases in the final few rays (Figs. 3 and 4). Finally, DF and AF show weak symmetry: while the patterns of length and segmentation showed similar position effects, differences in magnitude created significant fin effects and position × fin interactions. Implications of these findings, combined with observations on fin-ray mobility and flexibility, are presented below.

**Spines.** Change in spine length did not necessarily correlate with lateral mobility or stiffness. Instead, the difference in mobility and stiffness/flexibility may be due to the robustness of the spine and its articulation with its pterygiophores. Although all spines appeared to have a tight articulation with the underlying pterygiophores (Fig. 2C), the length and robustness of the corresponding radials, as well as the thickness of the spines, decreased with position, which we would suggest as a potential reason the posterior DSps were the most susceptible to lateral deflection and bending. It is not known whether the force required to achieve lateral deflection or bending would occur during normal swimming behaviors. We suggest that the spiny dorsal fin could be divided into two functional regions: the anterior region of the fin, supported by spines 1–4, acts as a cutwater, dividing the flow of water to either side of the fin with minimal disturbance to the direction of flow. In contrast, the posterior region of the fin, supported by spines 4–10, acts as a keel to provide either roll and/or yaw stability to the anterior region of the trunk, particularly during maneuvering (Fig. 14).

Although the three ASps are located more caudally along the longitudinal axis of the fish than the anterior four DSps, preventing any statistical comparison between fins, the similarity in skeletal features nonetheless suggests that the spiny region of the AF also acts primarily as a cutwater (Fig. 14). However, due to its small surface area, the ability of the spiny region to act as a keel and provide stability may be severely reduced.

**Rays.** As curvature occurs within the Sg region of the rays, with bending thought to be confined to the joints between adjacent segments (Alben et al., 2007), rays with absolutely and relatively greater segmentation should be capable of curvature over more of their length. From the length vs. ray position pattern we observed, we would expect the point along the RL where curvature is initiated to move proximally with longitudinal position (Figs. 3 and 4B) with the middle rays having the greatest proportion undergoing curvature (Fig. 4D). It is

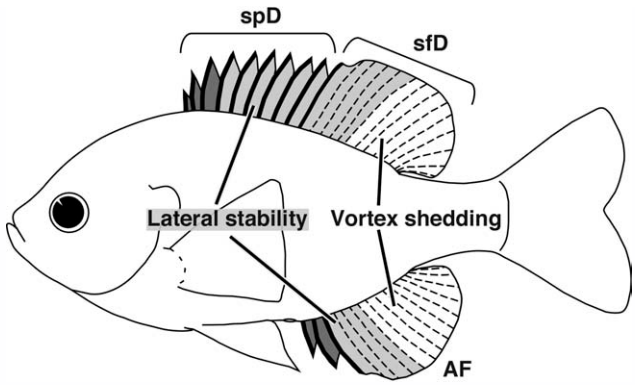


Fig. 14. Proposed median fin regionalization in bluegill. The shaded portions of the dorsal and anal fins represent areas suggested to provide lateral stability during swimming and maneuvering, with the darkest portions showing the regions that may act primarily as a cutwater. The unshaded areas, with fin rays directed primarily posteriorly, are suggested to be responsible for shedding vortices that assist propulsion. The suggested borders between stability- and thrust-producing regions were located at the inflection points of the graphs relating position to musculoskeletal parameters.

currently unknown whether the Br portions of the fin rays differ in their flexibility from the UBr portions, or if the branching is simply to support a greater expanse of fin membrane while retaining the same bony mechanical properties. Our finding of similar patterns in the Sg and Br portions of the rays suggests the latter, though this has not been tested explicitly.

Overall, the mobility (the degree of motion at the joint) and flexibility (the compliance of the ray to bending forces) increases caudally among rays. The increased mobility of the posterior rays during manipulation at the ray-pterygiophore joint matches our observation of a loose connection between the distal radial and its socket (Fig. 1B), which allows for lateral rotation about the longitudinal axis (Geerlink and Videler, 1973). Therefore, the anterior rays, where the distal radials have a tighter attachment with their sockets, should have a lesser degree of mobility in lateral deflection, supporting our contention that the anterior region functions primarily as a keel, providing lateral stability.

As with mobility, the anterior rays are more resistant to lateral bending forces, whether applied against the fin surface (simulating external forces) or by pulling on one head of the isolated ray (simulating intrinsic muscular forces). A potential explanation may be the tighter attachment between the two hemitrichia of the anterior rays (Fig. 6). As the degree of attachment increases, the capability of the fish to use muscular force alone to either induce ray curvature or actively resist bending forces applied externally would be diminished, if not impossible. This qualitative connection between the variation in ray stiffness and degree of curvature matches similar findings described in goldfish (Arita, 1971). Because of the imprecise nature of our manipulations, future experiments using more sophisticated and precise techniques (as seen in Alben et al., 2007) are required to accurately measure and confirm these preliminary findings.

Studies of fin-ray curvature in swimming fish have noted diverse patterns of curvature in paired and median fins. In the pectoral fin of longhorn sculpin, maximal curvature was found to be greatest at the proximal and distal ends and least in the midsection of the rays during station holding and steady swimming with maximum curvature varying among the rays (Taft et al., 2008). During steady swimming and slow turning maneuvers in bluegill, variations in curvature (measured at maximum fin excursions) along the DRy and ARy lengths, as well as between rays, were observed; however, no patterns in the position of maximum curvature were reported (Standen and Lauder, 2005). In our own study of ray curvature during C-starts (Chadwell, unpublished data), we found that the magnitude and position of maximum curvature along the RL varied over time but maximum ray curvature over the entire sequence generally occurred within the distal regions of the rays (i.e., the Br and Sg regions). Further studies combining quantitative kinematic data with morphology (e.g., Taft et al., 2008; Taft, 2011) are needed to fully understand the function of flexible fins during various behaviors in diverse species.

It is likely that the point of maximal bending is not relegated to a single location but rather is a function of the interactions among the intrinsic mechanical properties of the rays, hydrodynamic loading, movement of neighboring fin-rays and muscular activity at a given point in time. Therefore, how the position effects we found in segmentation and branching influences the location and degree of maximum bending under different forces is unclear. However, as ray bending should occur primarily within the Sg region (Alben et al., 2007), and both the absolute and percent length of the Sg regions increases with ray position (Figs. 3 and 4), we suggest that ray curvature in the proximal region of the ray (i.e., near the body) should be minimal.

## Muscular Regionalization

We reasoned that for each fin, erector muscles should be largest in the anterior regions, as the fin membrane connecting the fin-rays would passively pull on more posterior regions, and conversely, that depressor muscles would be largest in the posterior portions of the fin. In the context of splaying the fin, this would make sense. Simply erecting all the rays together would do little to increase the surface area of the fin; however, elevating the anterior rays while concurrently depressing the posterior ones would open the fin and their opposing actions would stretch the fin causing the surface to tighten, much like a collapsible hand fan. We found the expected pattern in the soft dorsal and anal fins (Figs. 9 and 10), and in the erectors, but not depressors, of the spiny dorsal fin (Figs. 7 and 8).

We further predicted that muscle masses would be correlated with fin-ray length, as a longer lever arm requires more force to move it, or resist an external applied force. We found significant positive correlations for all three muscles in the DRys and ARys, but not in the spines (Fig. 13). Potential functional implications of these findings are discussed below.

**Spines.** We suggest that the principal role of the erector muscles, to elevate the DSps, is more pronounced in the anterior than the posterior region. As elevation of posterior spines can occur passively when anterior spines are erected, the amount of force from the spine's own musculature required to elevate it would decrease posteriorly.

Depression of the spines appears to play an equal role within both regions of the spiny dorsal fin.

The role that inclinators play in resisting/initiating lateral movement of the spines is suspect due to the restricted mobility of their joint, as evidenced by the reduction or loss of spine muscles among several species (Winterbottom, 1974). Nonetheless, the persistence and increase in size of mInc among the posterior DSps of the bluegill suggests that these spines may experience more lateral deflection. Potentially, mInc of the posterior DSps could act to either counteract or generate hydrodynamic forces and/or provide intra-fin forces to control the lateral deflection of the anterior rays of the soft dorsal fin.

As with the skeletal features, the pattern of the spine musculature of ASp qualitatively matches the pattern observed among the anterior four spines of the spD, suggesting that the spiny portion of the AF is morphologically similar to the anterior region of the spiny dorsal fin. As the AF spines and their pterygiophores were larger and more robust than those of their dorsal fin counterparts (Fig. 3A,B), the absolute mass of their musculature was also larger, particularly mErec and mInc (Fig. 7), suggesting a need for more muscular force to counteract hydrodynamic loading at the AF.

The lack of correlation between spine length and mErec mass (Fig. 13A) supports our suggestion that the anterior spines of the dorsal fin carry a heavier load in elevating the spiny dorsal fin. Despite being the shortest spines (Fig. 3A), the mass of mErec for the first three spines are nearly equal to, if not larger than, those found among the longer posterior spines (Figs. 7A and 8C). Though spine length is moderately correlated with mInc, the correlation between spine position and mInc is much higher (Fig. 8), suggesting that the posterior spines require more muscle mass to either resist lateral deflection and/or provide support to the anterior rays of the soft dorsal fin.

**Rays.** Anterior–posterior regionalization of the soft portion of the DF and AF is supported by the expected significant position effects in rErec and rDepr (Figs. 9C,D and 10), consistent with splaying of the fin membrane. In contrast, the lack of significant position effect for rInc (Fig. 10E) suggests that the role for resisting (or initiating) lateral deflection is uniform over the expanse of the soft fins. Although muscle mass is a predictor of force, future studies should additionally measure the moment arm of the associated muscles to include any potential effects of variation or regionalization in lever mechanics.

Unlike the spines, muscle mass within the soft DF and AF is strongly correlated to RL (Fig. 13), with no rays showing a disproportionate increase or decrease in their muscle complement. Assuming equal pressure across the fin, longer rays should be supporting a larger area of the fin surface and thus greater forces acting on them, requiring more muscle force to resist/overcome the forces (Force = Area $\times$ Pressure).

### Dorsal Versus Anal Rays

For all variables tested, both skeletal and muscular, any significant position effects found in both fins were found to be equivalent between groups. Therefore, patterns of musculoskeletal design are highly conserved between the DF and AF. Significant fin $\times$ position interactions were found in all but one ($\Delta$mDepr) of the raw variables tested. Within the anterior regions, ARys were larger than their corresponding DRys, while the posterior DRys were either larger than or equal to their AF counterparts (Figs. 5 and 11). We suggest that this interaction is a result of an obvious difference between the two soft fins, i.e., the large spD vs. the smaller spiny region of the AF. For the soft dorsal fin, the 10 spines of the spiny dorsal fin can act as the cutwater and keel to keep the oncoming flow steady and provide support to the rays, particularly in the anterior region. In the AF, only three spines are present to act as the cutwater and keel; as such, the musculoskeletal features of the anterior anal fin-rays are disproportionately large and robust to compensate for the reduced support of spines. The size differences observed may be necessary for the DF and AF to produce vortices of the same magnitude (Tytell, 2006).

### Fin Regionalization and Locomotor Function

Hydrodynamic studies of steady swimming in bluegill have shown that both the soft dorsal and anal fins produce vortices in their wake oriented to create primarily lateral forces, but also include a thrust component that accounts for up to 14% each of the total thrust generated by the fish (Drucker and Lauder, 2001; Tytell, 2006). Moreover, these vortices have been suggested to interact with the caudal fin to further increase thrust generated by the tail (Tytell, 2006). The DF and AF also produce vortices that are integral contributors to the performance of the C-start (Tytell and Lauder, 2008). During steady swimming, lateral forces generated by the two fins are oriented in the same direction, providing counterbalance to any roll perturbations to the body (Drucker and Lauder, 2001, 2005; Standen and Lauder, 2005, 2007; Tytell and Lauder, 2008). Thus, the DF and AF of bluegill are playing multiple roles: stabilizing lateral forces and producing additional thrust.

While whole fin measurements provide basic comprehension of how the fins interact with the surrounding fluid, understanding variation between the rays of the fin generates additional insight, as has been shown for the pectoral fin of

sculpin (Taft et al., 2008; Taft, 2011). The division of the DF and AF into two regions (anterior and posterior) in a swimming fish (Fig. 14) is supported by an immediately obvious difference: the rays of the anterior region, particularly in the dorsal fin, are held to a higher degree of elevation, and thus the less mobile and stiffer anterior rays may be acting as an extension of the spiny fin, keeping the flow of water steady and guiding it to the more mobile and flexible posterior region. In contrast, the angle of elevation of the posterior rays decreases to near parallel to the long axis and their distal ends form the trailing edge of the fins, which shed the wake vortices (Fig. 14). Based on their greater segmentation, the more flexible posterior rays should be capable of fine-tuning their stiffness and orientation relative to the body to appropriately direct the flow for the desired swimming behavior. As shown by Tytell (2006), the vortices generated by the two median fins not only supply thrust forces independently, but they are positioned in time and space to interact downstream with the caudal fin, which appears to enhance the thrust generated by the tail during swimming. Thus, our morphological findings suggest that the anterior and posterior median fin regions may play functionally different roles during locomotion.

## ACKNOWLEDGMENTS

The authors would like to thank Dr. Anita McCauley for assistance with photographing specimens and Ben Hunter for assistance with data collection. Two anonymous reviewers provided comments that substantially improved the paper.

## LITERATURE CITED

Alben S, Madden PG, Lauder GV. 2007. The mechanics of active fin-shape control in ray-finned fishes. J R Soc Interface 4:243–256.

Arita GS. 1971. A re-examination of the functional morphology of the soft-rays in teleosts. Copeia 1971:691–697.

Blake RW. 2004. Fish functional design and swimming performance. J Fish Biol 65:1193–1222.

Drucker EG, Lauder GV. 2001. Locomotor function of the dorsal fin in teleost fishes: Experimental analysis of wake forces in sunfish. J Exp Biol 204:2943–2958.

Drucker EG, Lauder GV. 2005. Locomotor function of the dorsal fin in rainbow trout: Kinematic patterns and hydrodynamic forces. J Exp Biol 208:4479–4494.

Eaton TH, Jr. 1945. Skeletal supports of the median fins of fishes. J Morphol 76:193–212.

Geerlink PJ, Videler JJ. 1973. Joints and muscles of the dorsal fin of *Tilapia nilotica* L. (Fam. Cichlidae). Neth J Zool 24:279–290.

Geerlink PJ, Videler JJ. 1987. The relation between structure and bending properties of teleost fin rays. Neth J Zool 37: 59–80.

Goodrich ES. 1904. On the dermal fin-rays of fishes - Living and extinct. Q J Microsc Sci 47:465–522.

Haas HJ. 1962. Studies on mechanisms of joint and bone formation in the skeleton rays of fish fins. Dev Biol 5:1–34.

Hoogland R, Morris D, Tinbergen N. 1956. The spines of sticklebacks (*Gasterosteus* and *Pygosteus*) as means of defence against predators (*Perca* and *Esox*). Behaviour 10:205–236.

Lauder GV. 2006. Locomotion. In: Evans DH, Claiborne JB, editors. The Physiology of Fishes, 3rd ed. Boca Raton: CRC Press. pp 3–46.

Lauder GV, Madden PGA. 2007. Fish locomotion: Kinematics and hydrodynamics of flexible foil-like fins. Exp Fluids 43:641–653.

Mabee PM, Aldridge E, Warren E, Helenurm K. 1998. Effect of clearing and staining on fish length. Copeia 1998:346–353.

Mabee PM, Crotwell PL, Bird NC, Burke AC. 2002. Evolution of median fin modules in the axial skeleton of fishes. J Exp Zool 294:77–90.

McCutchen CW. 1970. The trout tail fin: A self-cambering hydrofoil. J Biomech 3:271–272.

Rasband WS. 2008. ImageJ. Version 1.41g. Bethesda, MD: U.S. National Institutes of Health. available at: http://rsb.info.nih.-gov/ij/. Accessed on 3 March 2008.

Rice WR. 1989. Analyzing tables of statistical tests. Evolution 43:223–225.

Sokal RR, Rohlf FJ. 1981. Biometry. New York: WH Freeman. p 805.

Song JK, Parenti LR. 1995. Clearing and staining whole fish specimens for simultaneous demonstration of bone, cartilage, and nerves. Copeia 1995:114–118.

Standen EM, Lauder GV. 2005. Dorsal and anal fin function in bluegill sunfish *Lepomis macrochirus*: Three-dimensional kinematics during propulsion and maneuvering. J Exp Biol 208:2753–2763.

Standen EM, Lauder GV. 2007. Hydrodynamic function of dorsal and anal fins in brook trout (*Salvelinus fontinalis*). J Exp Biol 210:325–339.

Taft,NK. 2011. Functional implications of variation in pectoral fin ray morphology between fishes with different patterns of pectoral fin use. J Morphol 272:1144–1152.

Taft NK, Lauder GV, Madden PGA. 2008. Functional regionalization of the pectoral fin of the benthic longhorn sculpin during station holding and swimming. J Zool 276:159–167.

Tytell ED. 2006. Median fin function in bluegill sunfish *Lepomis macrochirus*: Streamwise vortex structure during steady swimming. J Exp Biol 209:1516–1534.

Tytell ED, Lauder GV. 2008. Hydrodynamics of the escape response in bluegill sunfish, *Lepomis macrochirus*. J Exp Biol 211:3359–3369.

Videler JJ. 1977. Mechanical properties of fish tail joints. Fortsch Zool 24:183–194.

Walker JA. 2004. Kinematics and performance of maneuvering control surfaces in teleost fishes. IEEE J Oceanic Eng 29:572–584.

Winterbottom R. 1974. A descriptive synonymy of the striated muscles of the Teleostei. Proc Acad Nat Sci Phila 125: 225–317.

Zar JH. 1984. Biostatistical Analysis. Englewood Cliffs: Prentice-Hall. p 469.